Title

Modeling transport in fractured porous media with the random-walk particle method: The transient activity range and the particle-transfer probability

Journal

Water Resources Research, 38(6)

Authors

Pan, Lehua
Bodvarsson, Gudmundur S.

Publication Date

2001-05-30

Modeling transport in fractured porous media with the random-walk particle method: The transient activity range and the particle-transfer probability

Lehua Pan and Gudmundur S. Bodvarsson

Earth Sciences Division
Lawrence Berkeley National Laboratory
Mail Stop: 90-1116
One Cyclotron Road
Berkeley, CA 94720

Abstract

Multiscale features of transport processes in fractured porous media make numerical modeling a difficult task, both in conceptualization and computation. Modeling the mass transfer through the fracture-matrix interface is one of the critical issues in the simulation of transport in a fractured porous medium. Because conventional dual-continuum-based numerical methods are unable to capture the transient features of the diffusion depth into the matrix (unless they assume a passive matrix medium), such methods will overestimate the transport of tracers through the fractures, especially for the cases with large fracture spacing, resulting in artificial early breakthroughs. We have developed a new method for calculating the particle-transfer probability that can capture the transient features of diffusion depth into the matrix within the framework of the dual-continuum random-walk particle method (RWPM) by introducing a new concept of activity range of a particle within the matrix. Unlike the multiple-continuum approach, the new dual-continuum RWPM does not require using additional grid blocks to represent the matrix. It does not assume a passive matrix medium and can be applied to the cases where global water flow exists in both continua. The new method has been verified against analytical solutions for transport in the fracture-matrix systems with various fracture spacing. The calculations of the breakthrough curves of radionuclides from a potential repository to the water table in Yucca Mountain demonstrate the effectiveness of the new method for simulating 3-D, mountain-scale transport in a heterogeneous, fractured porous medium under variably saturated conditions.

1. Introduction

Transport through fractured porous media occurs in many subsurface systems and is of great importance in many scientific and engineering fields (e.g., underground natural resource recovery, waste storage, soil physics, and environmental remediation). In fractured porous media, the fractures generally occupy a tiny portion of the whole volume, but the pore-water velocity in these fractures can be orders of magnitude higher than that in the matrix (Wu et al., 2000). At the same time, especially under variably saturated conditions, the global water flow in the matrix and the mass exchange between the fractures and the matrix also play important roles in the transport process. These special features distinguish the fractured porous media from general heterogeneous porous media or pure fracture networks (without porous matrix), and make many numerical methods for treating heterogeneity unsuitable. In modeling transport in a fracture-matrix system, mass transfer between the fractures and the matrix is one of the key modeling issues (Neretnieks, 1980; Sudicky and Frind, 1982; Barker, 1985; Pruess and Narasimhan,1985; Maloszewski and Zuber, 1993; Wu and Pruess, 2000; Liu et al. 2000; and Tsang and Tsang, 2001, among others). Except for a few simple cases, analytical solutions are not available for the mass transfer between the fractures and the matrix. A discrete-fracture-network model with a finely gridded matrix is not feasible for most real-world problems. As a result, numerical methods based on the dual-continuum approache have often been used to simulate the fracture-matrix transport system (Huyakorn et al., 1983; van Genuchten and Dalton, 1986; Liu et al., 2000; Wu and Pruess, 2000, among others). The major advantage of the dual-continuum approach is its

capability to capture the major features of flow and transport in fractured porous rock (i.e., a fast fracture subsystem combined with a slow matrix subsystem) with reasonable computational resources. However, the dual-continuum approach does not generally capture the transient features of the diffusion depth into matrix because a single grid block is used to represent the matrix. In many cases, especially with large fracture spacing, a poor estimation of the diffusion flux through the fracture-matrix interface (because of missing such transient features) may lead to significant errors in predicted breakthrough curves (Figure 1). Figure 1 shows an example of the simulated breakthrough curves from a system of parallel fractures separated by porous media. The dual-continuum-based method is the conventional dual-continuum random-walk particle tracking method (DCPT V1.0) while the analytical solution is based on the solution derived by Sudicky and Frind (1982). Obviously, the dual-continuum-based method greatly overestimates the breakthrough at early time. To address this problem, a more general "multiple-interacting continua" (MINC) method was proposed for finite difference methods by Pruess and Narasimhan (1985), which uses a number of nested matrix blocks to capture the transient features of diffusion depth into the matrix. Obviously, the MINC approach requires more (e.g., often 10 times more) grid cells than the dual-continuum approach (Wu and Pruess, 2000). This would result in a higher computational cost (comparable with the cost of a discrete-fracture-network model) that makes it unfeasible for large-scale problems. Recently, Tsang and Tsang (2001) proposed an approach to simulate the diffusion into finite matrix blocks for the residence-time particle tracking method based on an analytical solution for a simplified fracture-matrix system. However, the method is applicable only for the cases in which the matrix can be

assumed to be passive medium (i.e., no water flow in the matrix or through the fracture-matrix interface), which may oversimplify many real-world problems, especially where unsaturated conditions prevail.

In this paper, we present a new technique for simulating transport in 3-D, fractured porous media using the random-walk particle-tracking method. The new technique is an extension and improvement of previous approaches (Pan et al., 2001). The main advance is the development of a new method for calculating the particle-transfer probability, which captures the transient features of diffusion depth into matrix within the dual-continuum framework. As a result, the proposed dual-continuum RWPM still maintains the simplicity and high efficiency of the RWPM without the disadvantages of the conventional dual-continuum approach.

2. Theory and methods

2.1 Dual-continuum approach

In the dual-continuum approach, the fractured porous medium is represented with two interacting continua: a fracture continuum and a matrix continuum. In our dual-continuum model, the entire domain is discretized into grid cells with each cell containing both continua. Each continuum is connected individually between adjacent cells while two continua are connected via the fracture-matrix interface within each cell. Two flow fields are defined for two continua, respectively, and additional water fluxes within each cell are used to describe the water flow between the two continua. Such 4-D flow fields (3-D plus fracture-matrix dimension) can be calculated, for instance, by using finite-difference or finite-element methods with a dual-continuum grid. The transport

process is also split into two sub-transport-processes in each continuum and the mass exchange process between two continua within each cell.

2.2 Dual-continuum RWPM

There are many random-walk particle method (RWPM) algorithms available in the literatures (Labolle et al., 1996, 2000; Tompson and Gelhar, 1990; Uffink, 1985; Semra et al., 1993; and many others) for simulation of transport in a single-continuum medium, which will not be discussed here. The dual-continuum RWPM used here is similar to the approach proposed by Liu et al. (2000) except for that a different time stepping strategy is used. It simulates the particle movements in each continuum with regular (single-continuum) RWPM and uses a random continuum-switch process to simulate the particle transfer between two continua (Pan et al., 2001). A random number is drawn from the uniform distribution U[0, 1] and compared to the particle-transfer probability after each movement. If the random number is larger than the particle-transfer probability, the other continuum will be selected as the medium in which the particle will travel at the next time step. Otherwise, the current continuum is still the selected medium. In this way, particles will travel randomly in either fractures or matrix.

The dual-continuum RWPM tracks both the location (including which continuum) of each particle and the time spent to reach that location. As a result, we can derive a breakthrough curve by calculating the total mass carried by the particles passing a specified observation location (e.g., at water table) at different times. If all particles are released at the same time, the breakthrough curve will correspond to a tracer pulse injection. By defining appropriately the particle release times at the source, we can

calculate the breakthrough curves for any given tracer injection with variable concentration.

2.3 Particle-Transfer Probability: The Conventional Approach

The particle-transfer probability is here defined as the probability of a particle entering another continuum during a given time interval. Because the fracture-matrix interaction is described at the cell level in the dual-continuum model, the particle-transfer probability is also calculated at the cell level for each continuum. The net mass transfer from the fracture continuum to the matrix continuum during the time interval Δt is the difference between the mass transferred from the fractures to the matrix (m_{fm}) and the mass transferred from the matrix to the fractures (m_{mf}) during the same time interval. It can be related to the particle-transfer probability as follows:

$$m_{fm} - m_{mf} = N_f \, \mu \, P_{fm} - N_m \, \mu \, P_{mf} \qquad (1)$$

where, μ is the mass carried by each particle while P_{fm} and P_{mf} are the particle-transfer probabilities for particles in the fracture and the matrix continua at time t, respectively. The subscript indicates the transfer direction (e.g., "fm" means from the fracture continuum to the matrix continuum). N_f and N_m are the numbers of particles in the fracture continuum and the matrix continuum, respectively, for a given cell at time t. Unlike finite-difference methods or finite-element methods, the particle-tracking method does not directly calculate the net mass transfer between two continua. Instead, it

simulates the mass transfer in two directions separately by tracking the transfer of the particles between two continua. For example, particle transfer occurs even if the net mass transfer equals zero between the two continua, which only means that the number of particles transferred is the same in both directions. In other words, two terms in Equation (1) are simulated separately. Thus, the particle-transfer probability from one continuum to the other can be calculated as the ratio of the mass entering the other continuum during the time interval, Δt, to the mass in the current continuum at the beginning of the time interval. Finding a proper scheme to estimate the mass transfer between two continua (m_{fm} or m_{mf}) is essential. The mass transfer consists of two components: advection and diffusion/dispersion. The component due to advection can be directly calculated as the product of the amount of the water entering the other continuum and the concentration of that water. The component due to diffusion/dispersion, however, needs to be calculated based on some assumptions about the concentration distribution within the matrix because only a single grid block is used to represent the matrix in a dual-continuum model. By assuming a second-order polynomial distribution of concentration away from the fracture-matrix interface into the matrix, Liu et al. (2000) proposed a simple scheme to approximate the diffusion component of the mass transfer and the corresponding particle transfer probabilities for both directions. However, the scheme may fail if Δt is large. To overcome the problem, Pan et al. (2001) have derived an improved scheme by considering the temporal feature of the average concentration (Appendix A). The new schemes of P_{fm} and P_{mf} for a given time interval, Δt, can be calculated as (2a) and (2b), respectively (see Appendix A).

$$P_{fm} = \frac{F_{fm}}{Q_f + F_{fm}}[1-\exp(-\Delta t/\tau_f)] \qquad (2a)$$

$$P_{mf} = \frac{F_{mf}}{Q_m + F_{mf}}[1-\exp(-\Delta t/\tau_m)] \qquad (2b)$$

where F and Q describe the strength of advection and dispersion/diffusion processes through the fracture-matrix interface and the interfaces to adjacent grid cells in the same continuum, respectively. The subscripts indicate the direction of those processes. The parameters τ_f and τ_m are the characteristic times of the fracture continuum and the matrix continuum, respectively. The detailed expressions of these parameters are listed below:

$$F_{fm} = \max(q_{fm}A_{fm},0) + \frac{D_m A_{fm}}{S_{fm}} \qquad (3a)$$

$$Q_f = \sum_{i=1}^{N}\left[\max(q_f A_i,0) + \frac{Df_i A_i}{S_i}\right] \qquad (3b)$$

$$\tau_f = \frac{V_f R_f}{F_{fm} + Q_f} \tag{3c}$$

$$F_{mf} = \max(-q_{fm} A_{fm}, 0) + \frac{D_m A_{fm}}{S_{fm}} \tag{3d}$$

$$Q_m = \sum_{i=1}^{N} \left[\max(q_m A_i, 0) + \frac{Dm_i A_i}{S_i} \right] \tag{3e}$$

$$\tau_m = \frac{V_m R_m}{F_{mf} + Q_m} \tag{3f}$$

where, A_{fm} and A_i are the area of the effective fracture-matrix interfaces within the grid cell and the interface area to the ith adjacent grid cell, respectively. The q_{fm} (positive if flow from the fracture to the matrix) and q_i (outwardly positive) are the water flux through the fracture-matrix interface within the grid cell and the interface to the ith adjacent grid cell, respectively. The parameters D_m , Df_i, and Dm_i are effective dispersion coefficients of the matrix within the grid cell, the fracture continuum at the interface to the ith adjacent cell, and the matrix continuum at the interface to the ith adjacent cell, respectively. S_i is the distance between the center of the cell and the ith adjacent cell, while S_{fm} is the characteristic length of the fracture-matrix system (e.g., 1/6 of the fracture spacing for a parallel fracture system as suggested by Liu et al., 2000). V and R are the volume of water and the retardation factor, respectively, with the subscripts

indicating the continuum. Note that for a very small time step ($\Delta t/\tau_f$ or $\Delta t/\tau_m$ reaches to zero), the particle-transfer probabilities defined in Equations (2a) and (2b) will reduce to the expresion proposed by Liu et al. (2000).

The scheme defined in Equation (2a) and (2b) with (3a-f) has been implemented in a code called DCPT V1.0 (Pan et al., 2001).

2.4 Particle-Transfer Probability:The Transient Effect and The Activity Range

In the remainder of the paper, we shall consider only the case of tracer injection with a single concentration pulse at time 0, because in a particle-tracking method any given tracer injection with variable concentration can be simulated by a series of pulses appropriately arranged over times at the source, and the breakthrough curve can be calculated by summing up all individual breakthrough curves corresponding to the individual pulse injections. In fact, such a superposition calculation is straightforward in the dual-continuum RWPM proposed here because (1) any pulse can be represented by a certain number of particles released at the same time and (2) both the amount of mass and the time by which a particle reaches a particular location are tracked for each particle.

As shown in Figure 1, the scheme described in Equations (2) and (3) may lead to overestimating the breakthrough at early time for systems with large fracture spacing. To consider the problem, let us start with the parallel fracture system depicted in Figure 2 (the upper portion). After a pulse of particles is injected into the fractures at t = 0, the pulse will gradually spread into the matrix. At early times, the range of the particle cloud is limited, and only a tiny portion of the matrix is involved. Meanwhile, the concentration gradient at the fracture-matrix interface is much greater than that at later time. In terms of

random-walk particles, the distribution density function for the probability of finding a particle at any specific location away from the fracture-matrix interface becomes wider and flatter over time (lower portion of Figure 2, t3 > t2 > t1). The method described above, however, does not capture these transient features of the diffusion depth into the matrix for a given pulse. As a result, the method will underestimate the mass exchange between the two continua at early time and consequently overestimate the early breakthrough, because the pore-water velocity in the fractures is usually orders of magnitude faster than that in the matrix.

The problem with this method is that the full matrix volume, V_m, and the characteristic distance, S_{fm}, are used in calculating the particle-transfer probability regardless of the time while in reality both of them are time-dependent. To see the physical meanings of V_m and S_{fm} in the above method, we can rewrite the net mass-transfer rate from the fractures to the matrix, J_{fm}, as:

$$J_{fm} = \frac{N_f \mu}{V_f R_f} \max(q_{fm} A_{fm}, 0) - \frac{N_m \mu}{V_m R_m} \max(-q_{fm} A_{fm}, 0) + \frac{D_m A_{fm}}{S_{fm}} \left(\frac{N_f \mu}{V_f R_f} - \frac{N_m \mu}{V_m R_m} \right) \qquad (4)$$

Equation (4) is obtained by inserting Equations (2) and (3) into Equation (1) and then taking the derivative of Equation (1) with respective to Δt at $\Delta t = 0$. As shown in Equation (4), the characteristic distance S_{fm} is used to describe the steepness of the concentration gradient at the fracture-matrix interface, while the matrix volume V_m is used to define the concentration in the matrix for a given number of particles. As the result of a diffusion process, the concentration gradient decreases and the volume of the matrix that contains the particles increases with time, after a pulse is injected in the

fracture. Both phenomena are caused by the limited, yet advancing, diffusion depth into the matrix. In terms of the random-walk method, the walks of particles are confined within a certain range in the matrix, depending on the time elapsed since the pulse has been injected. We call such a range the activity range of particles, which can be defined for each individual pulse such that the probability of finding a particle of the pulse outside the range is practically zero. Obviously, the activity range is a function of time elapsed since the injection of the pulse, t_p, which can be tracked as the age of a particle in the dual-continuum RWPM. This is because it is the time elapsed since the particle is injected (born) into the fracture continuum. To incorporate these transient features in the dual-continuum RWPM, we propose to modify the particle-transfer probability by replacing the characteristic distance S_{fm} and the matrix volume V_m in (3a), (3d) and (3f) with the effective characteristic distance $S_{fm}(t_p)$ and the effective matrix volume $V_m(t_p)$. These parameters are related to the activity range as follows:

$$S_{fm}(t_p) = S_{fm}\frac{B^*(t_p)}{B} \tag{5a}$$

$$V_m(t_p) = V_m\frac{B^*(t_p)}{B} \tag{5b}$$

where, $B^*(t_p)$ is the activity range, whose value varies from 0 to B, the maximum activity range (e.g., one-half of the fracture spacing as defined in Figure 2 for a system of

parallel-plate fractures separated by porous rock). Note that the maximum activity range may be significantly less one-half of the fracture spacing under unsaturated flow condition even for a parallel fracture system because only a portion of connected fractures is active (Liu et al., 1988). For a fractured porous medium with more complicated geometry configurations, the relationship between the maximum activity range and the fracture spacing cannot be expressed in a simple way. To be general, we suggest that the maximum activity range, B, be approximated as the ratio of the volume of matrix, V_m, to the area of the effective fracture-matrix interfaces within a given grid cell, A_{fm}, for an arbitrary fracture-matrix system under varied saturated conditions. Here, A_{fm} is determined as the product of the fracture-matrix interface area calculated based on the geometry of the fracture network and the fracture-matrix-interface-area-reduction-factor proposed by Liu et al. (1998).

To develop a method for estimating the activity range $B^*(t_p)$ for a particle, we can consider the transport in a system of parallel-plate fractures separated by porous rock responding to a pulse injection in the fractures (Figure 2). By the superposition principle, only the 1-D governing equation (in the fracture-matrix dimension) is needed to derive the activity range:

$$\frac{\partial}{\partial t_p}[RC]=\frac{\partial}{\partial s}\left(D_m \frac{\partial C}{\partial s}\right) \tag{6}$$

where s is the distance into the matrix. A pulse injection of tracer at t = 0 are confined in the fractures (and ignoring the fracture aperture b because b<<B) and can be expressed as follows:

$$C(s,0) = M_s \sum_{i=0}^{\infty} \delta(s - 2iB) \tag{7}$$

where $\delta(\bullet)$ is a Dirac delta function, whose value is zero everywhere except for infinite value at point zero, which describes pulse injections at the fractures only while i is the index of fractures. The term M_s is a scaling factor that makes the C in the final solution equivalent to the probability to find a particle at any specific location away in the matrix (a dimensionless variable within a range between 0 and 1). The solution to Equation (6) subject to Equation (7) can be expressed as (for $s \geq 0$ and using symmetry, Bear, 1972):

$$C(s,t_p) = \frac{2M_s}{(4\pi D_m t_p/R_m)^{1/2}} \sum_{i=0}^{\infty} \exp\left(-\frac{(s-2iB)^2}{4D_m t_p/R_m}\right) \tag{8}$$

For a very small time,

$$C(s,t_p) = \frac{2M_s}{(4\pi D_m t_p/R_m)^{1/2}} \exp\left(-\frac{s^2}{4D_m t_p/R_m}\right) \tag{9}$$

Because the concentration in Equation (9) can interpreted as the probability of finding a particle (initially at s=0) at location s and time t_p, the probability that a particle will be located in the activity range [0, B^*] can be obtained by integrating Equation (9) with respect to s from 0 to B^*:

$$P(0 \leq s \leq B^*) = \text{erf}\left(\frac{B^*}{\sqrt{4D_m t_p/R_m}}\right) \tag{10}$$

Equation (10) implies that B^* should be proportional to the square root of t_p. By definition, we should select a B^* such that $P(0 \le s \le B^*)$ is close to 1. An adequate activity range for short time can be expressed as:

$$B^*(t_p) = \min\left(4\sqrt{4 D_m t_p/R_m}, B\right) \tag{11}$$

The corresponding $P(|s| \ge B^*)$ is about 10^{-7}, and B is by definition the maximum activity range.

At a longer time, B^* approaches B, and the other terms in Equation (8) cannot be ignored. There is no simple solution such as Equation (9) for that case. However, because our purpose is to get a proper $B^*(t_p)$, we can assume that the relative effects of the other terms in Equation (8) on the activity range are equal to their relative contributions to the concentration. In other words, the activity range can be modified as follows:

$$B^*(t_p) = \min\left(4\sqrt{4 D_m t_p/R_m}\, W(t_p), B\right) \tag{12}$$

The weighting function $W(t_p)$ is derived as the ratio of the two-term solution to the one-term solution as defined in Equation (8) at a given B^*. It can be approximated as:

$$W(t_p) \approx \sum_{i=0}^{1} \exp\left[-\frac{\left(B^* - 2iB\right)^2}{4 D_m t_p/R_m}\right] \Bigg/ \exp\left[-\frac{B^{*2}}{4 D_m t_p/R_m}\right] \approx 1 + \frac{1}{1 + \frac{B\left(B - B^*\right)}{D_m t_p/R_m}} \tag{13}$$

The reason for taking only two terms in calculating the weighting function is because further terms are insignificant for typical values of B.

The water flow through the fracture-matrix interface may act to increase the activity range (if flow is from the fractures to the matrix) or decrease it (if flow is from the matrix to the fractures). In a dual-continuum model, however, we only know the flux at the fracture-matrix interface. Numerical experiments (not shown here) show that this effect is not significant because the diffusion component would be less important if the water flow through the fracture-matrix interface were large and the effects of that water flow on the particle-transfer probability have already been incorporated separately. We simply assume that the effect of water flow through the fracture-matrix interface on the activity range is limited within a thin skin of the interface. As a result, the activity range can be modified as:

$$B^*(t_p) = \min\left(4\sqrt{4 D_m t_p / R_m}\, W(t_p) + \mathrm{sign}(q_{fm}) \max\left(\frac{|q_{fm}|\, t_p}{\theta_m}, 2b \right), B \right) \qquad (14)$$

where 2b is the effective fracture aperture and θ_m is the volumetric water content in the matrix.

3. Implementation Issues

3.1 The Framework of Dual-Continua RWPM

In the dual-continuum RWPM proposed here, particles travel in continuous 3-D space. However, the domain is discretized into a limited number of grid cells. Each cell contains a fracture continuum and a matrix continuum. All media parameters are assumed to be cell-wise constant for each continuum. A particle may travel randomly in either the fractures or the matrix. For each step, the particle tracker first determines how long (i.e.,

the time step) the particle will travel for the current step and whether or not the particle will transfer to the other continuum after this step. Then it uses a regular RWPM to determine the new location of the particle, using the parameters of the current continuum (Pan et al., 2001). An efficient cell-locator is used to determine which cell of the 3-D, irregular grid the particle resides in after each step. The proposed dual-continuum RWPM has been implemented in a code called DCPT v2.0. Note that the only difference of the dual-continuum RWPM implemented in DCPT v2.0 and DCPT v1.0 is that the particle-transfer probability is a function of a particle's age (t_p) in DCPT v2.0, but not in DCPT v1.0.

3.2 The Adaptive Time Stepping

Adequate time steps used in a simulation are very important for the accuracy of any RWPM because of its inherent explicit approach. We suggest using the following adaptive time-stepping technique to achieve high performance without losing accuracy:

$$\Delta t = 0.05 \min\left(\frac{\Delta xy}{|V^f xy|}, \frac{\Delta z}{|V^f z|}, \tau_f \right) \qquad \text{in fractures} \qquad (15a)$$

$$\Delta t = 0.05 \min\left(\frac{\Delta xy}{|V^m xy|}, \frac{\Delta z}{|V^m z|}, \tau_m \right) \qquad \text{in matrix} \qquad (15b)$$

where Δxy and Δz are the lateral size (square root of the area in xy-plane) and thickness of the given grid cell, respectivley. The parameters Vxy and Vz are the lateral and vertical components of the pore-water velocity vector, respectively. The superscript indicates the continuum. The parameters τ_f and τ_m are the characteristic times, defined in (3c) and (3f), for the fracture continuum and the matrix continuum of the given grid cell,

respectively. The main advantage of the time-stepping technique based on Equation (15) is to use small time steps only where it is necessary (e.g., at location having high pore-water velocity).

3.3 Calculation of the Activity Range

The activity range, B^*, is calculated with a two-step approximation: (1) to get a primary activity range using Equation (11) first, and (2) then use this primary estimation of the activity range to get a new activity range B^*, using Equation (14).

3.4 Exception of the Activity Range and the Initial Status

The above derivation of the activity range is valid only for particles initially released in the fractures. The activity ranges for particles released into the matrix would be different, and depend on how far from the interface they are initially located, which is not known in practice. We assume that all particles initially released into the matrix are uniformly distributed within the matrix, and thus the activity range will always be B. we assign a parameter called "initial status" to each particle to distinguish which continuum it is released into initially (at $t_p = 0$).

4. Results and Discussion

4.1 Verification with Analytical Solutions

An analytical solution for solute transport in fractured porous media with parallel fractures was derived by Sudicky and Frind (1982). This solution is based on the assumptions that (1) the solute transport between fractures and matrix occurs through

matrix diffusion in the horizontal direction only, and that (2) matrix advection and diffusion in the vertical direction can be ignored. Table 1 shows the relevant parameters for the two test cases. In particular, two different fracture spacings of 1 meter and 10 meters were used for Case 1 and Case 2, respectively.

Figure 3 shows the results for Case 1. Both old (DCPT v1.0) and new schemes (DCPT v2.0) predict breakthrough curves that agree well with the analytical solutions. The old scheme slightly overestimated the concentration at early times, but not very significantly for this small fracture spacing (1m). However, for Case 2, which has larger fracture spacing (10m), the old scheme seriously overestimates the breakthrough at early times (Figure 4). The plateau of the breakthrough curve predicted by the old scheme starts at about 0.1 year (beyond the scale in the figure). This means that more than 60% of solutes injected into the fractures at time zero would leach out of the system in about 0.1 year. But the analytical solution reveals that the similar time is about at 4×10^4 years. Note that the old scheme still agrees well with the analytical solution at very later time. On the other hand, the new scheme predicts breakthrough curves that are almost identical to the analytical solutions for both cases (Figure 3 and 4). Thus, the new scheme effectively solves the problem of capturing the transient features of the diffusion depth into the matrix using only one matrix block to represent the matrix in dual-continuum approaches.

The approach developed for the residence-time based particle tracking method requires assuming that the matrix acts as a passive medium only (Tsang and Tsang, 2001, among others). For finite-difference methods, a MINC approach was used to overcome the same problem, an approach that requires about 10 times more matrix blocks to

represent the matrix for typical fracture spacing (Pruess and Narasimhan, 1985; Wu and Pruess, 2000). Note that a similar approach based on the activity range concept can be incorporated into a finite-difference method if only a single pulse of tracers is simulated. However, it would not be applicable to the other types of problems because the mass in each grid cell cannot be labeled according to the injection times in a finite-difference method. Instead, it would have to decompose the problem into a number of subproblems of single pulse injection and then integrate the results of the subproblems one by one. The activity-range-based approach can be used for arbitrary fracture spacing without losing the simplicity and efficiency of the dual-continuum RWPM.

At early times, the fracture spacing should have little effects on the activity range because the activity range is controlled only by the diffusion process, and the weighting function $W(t_p)$ is almost one for a small t_p. The analytical solutions for Case 1 and Case 2 depicted in Figure 5 confirm this feature. Up to 5000 years, the breakthrough curves are almost identical for Case 1 and Case 2 (Figure 5).

To further explore the dynamics of the particle transfer between fractures and matrix, we have plotted the particle-transfer probabilities versus t_p in Figure 6 for a given time step (1 day). At very small t_p, the particle-transfer probabilities for both directions are close to 1, which indicates extensive mass exchange between the fractures and the matrix at that stage. With increasing t_p, the particle-transfer probabilities decrease quickly as the activity range in the matrix increases, until the activity range hits the maximum value (B), at which time the particle-transfer probabilities become constant. The turning age (t_p) for the case of 10 m fracture spacing is about 10^4 years, about 100 times that for the case of 1 m fracture spacing. This is consistent with the relationship expressed in

Equation (12), that t_p has a quadric relationship with B^*. The particle-transfer probability from the matrix to the fractures decreases faster than that from the fractures to the matrix, because the effective matrix volume also increases with the increase of the activity range but the effective fracture volume is constant. Conceptually, the particles in the matrix have a larger probability of staying far from the fracture-matrix interface as the activity range increases than the beginning, while the particles in the fractures are always close to the interface. The old scheme does not capture the dynamic feature of the particle-transfer probability described above and uses constant particle-transfer probabilities that are only valid for later times.

4.2 Application to Three-Dimensional Transport in Unsaturated Fractured Rocks

The unsaturated zone of Yucca Mountain is being considered as a potential subsurface repository for storage of high-level radioactive waste of the US. The potential repository would be located in the highly fractured Topopah Spring welded unit (TSw), about 300 m above the water table. An important issue in potential repository performance assessment is predicting the breakthrough of radionuclides at the water table in case of waste package failure. Computer modeling is the major approach for the task because the slow transport processes in unsaturated tuff could involve a temporal scale up to one million years.

The three-dimensional model domain and the corresponding irregular numerical grid of this mountain-scale problem are shown in plan view in Figure 7. The detailed descriptions of the model can be found in the related report written by Wu et al. (2000). The following is a summary. The model domain covers a total area of approximately 40

km^2. Domain thickness varies from 500 to 700 m, depending on local topography. The domain is filled with layered tuffs of spatially varied thickness complicated by faults. From the land surface downward, these layers are the Tiva Canyon welded (TCw) unit, the Paintbrush nonwelded (PTn) unit, the Topopah Spring welded (TSw) unit, the Calico Hills nonwelded (CHn), and the Crater Flat undifferentiated (Cfu) units. Fracture density varies with the different layers, mainly depending on the degree of welding. The potential repository is located in the middle of the domain, an approximate area of 1,000 m (east-west) by 5,000 m (north-south), surrounded by faults (Figure 7). The repository is represented by a number of 5 m thick grid cells. A steady-state flow field corresponding to the present-day infiltration map is assumed and calculated using the TOUGH2 code (Wu et al., 2000). The dual-permeability grid used in calculation has 104,156 grid cells and 421,134 connections. A pulse release of two radionuclides into fractures with technetium as a conservative tracer and neptunium as a reactive (i.e., adsorbing) tracer is considered. Table 2 shows the parameters used in the simulation. Radioactive decay and mechanical dispersion are ignored for simplicity.

Figure 8 and 9 show the predicted breakthrough curves at the water table for technetium and neptunium, respectively. In the figures, the relative mass is defined as the cumulative mass of the radionuclides passing through the water table over time, normalized by the total mass released at the repository. We also include the results generated by the finite-difference-based simulator, T2R3D, with a dual-continuum (dual-permeability) grid as a reference (Wu and Pruess, 2000). The same flow fields calculated using the TOUGH2 code are used for transport simulations with all three codes: T2R3D, DCPT V1.0, and DCPT V2.0. The CPU times used are about 3600 s for T2R3D on the

Alpha work station, 310 s for DCPT v1.0 on a Pentium PC, and 315 s for DCPT v2.0 on a Pentium PC. In both cases, DCPT v1.0 and T2R3D are in good agreement (Figure 8 and 9). This good match shows that the dual-continuum RWPM proposed by Pan et al. (2001) can be successfully applied to simulate the three-dimensional transport in the heterogeneous, unsaturated porous media. However, ignoring the transient feature of the diffusion depth into matrix have significantly affected the predicted breakthrough of radionuclides. Let us define t_{20} as the time by which 20% of the mass has passed through the water table. With the model proposed in this paper (DCPT v2.0), the predicted values of t_{20} are about 2,000 years for Tc (Figure 8) and 150,000 years for Np (Figure 9), respectively. Both DCPT v1.0 and T2R3D predict much smaller values of t_{20}, about 15 years for Tc (Figure 8) and 40,000 years for Np (Figure 9). The fast breakthrough represented by the first plateau in Figure 8 predicted by DCPT v1.0 and T2R3D is largely caused by overestimation of the transport through the fractures as a result of ignoring the transient features of the diffusion depth into matrix. Similar phenomena can be seen in Figure 9. Theoretically, this problem can be solved using a MINC mesh with T2R3D. However, the size of the required MINC mesh for such a mountain-scale application is practically prohibitive. For example, the fracture spacing in the TSw unit in which the repository located is about 0.31 m. The examples of using MINC meshes presented by Wu and Pruess (2000) show that eight sub-blocks are used for the case with 2B = 0.1 m and 11 sub-blocks for 2B = 0.17 m, respectively. As a result, the number of cells for a proper MINC mesh would at least be over a half-million, which may require a super computer to solve the same problem with parallel computing techniques (Wu et al., 2001). On the other hand, the particle tracking approach proposed here can solve this

problem for varied fracture spacing without using any additional grid blocks. Note that the active fracture model is applied in above unsaturated flow and transport simulations. Therefore, the fracture-matrix interface area varies greatly over space depending on the water saturation in the fracture continuum. As a result, the effective fracture spacing can be much larger than that calculated based on the geometry of the fracture network for a given formation of rock.

5. Summary

A new method for calculating particle-transfer probability between the fracture and matrix continua has been developed that captures the transient features of diffusion depth into matrix within the dual-continuum framework. As the result of a diffusion process, the concentration gradient decreases and the volume of the matrix containing the particles increases with time after a pulse of particles is injected into the fractures. In other words, the diffusion depth is limited and transient. In terms of the random walk method, all particles of that pulse will be confined within a limited range within the matrix (the activity range, which can be defined as the range in the matrix such that the probability of finding a particle outside the range is practically zero). The activity range of a particle is a function of the time elapsed since the pulse to which the particle belongs is injected, which can simply be tracked as the particle's age in a dual-continuum RWPM. As a result, the new dual-continuum RWPM can capture the important transient features of the diffusion depth into the matrix without using additional matrix blocks (as used in a multiple-continuum approach). It does not assume a passive matrix medium (as required by a residence-time particle-tracking approach) and can be applied to cases

where global water flow exists in both continua. It still maintains the simplicity and high efficiency of the RWPM without the disadvantage of the conventional dual-continuum approach. Results are in good agreement with existing analytical solutions with different fracture spacing. We have used this method to calculate breakthrough curves for radionuclide migrating from a potential repository to the water table in Yucca Mountain. The results of this calculation demonstrate the effectiveness of this new technique in simulating 3-D, mountain-scale transport in a heterogeneous, fractured porous medium under variably saturated conditions.

Acknowledgements

The authors would like to thank Karsten Pruess and Jianchun Liu for their internal review and thoughtful comments. This work was supported by the Director, Office of Civilian Radioactive Waste Management, U.S. Department of Energy, through Memorandum Purchase Order EA9013MC5X between Bechtel SAIC Company, LLC and the Ernest Orlando Lawrence Berkeley National Laboratory (Berkeley Lab). The support is provided to Berkeley Lab through the U.S. Department of Energy Contract No. DE-AC03-76SF00098.

References

Barker, J. A., Modeling the effects of matrix diffusion on transport on densely fissured media, Mem. Int. Assoc. Hydrogeol. 18:250-269, 1985.

Bear, J., *Dynamics of Fluid in Porous Media.* New York, New York: Dover Publications, 1972.

Huyakorn, P. S., B. H. Lester, and J. W. Mercer. An efficient finite element technique for modeling transport of fractured porous media. 1. Single species transport. Water Resources Research, 19:841-854, 1983.

Labolle, E. M., G. E. Fogg, and A. F. B. Tompson, Random-walk simulation of transport in heterogeneous porous media: Local mass conservation problem and implementation methods, Water Resources Research, 32:583-593, 1996.

LaBolle, E. M., J. Quastel, G. E. Fogg, and J. Gravner, Diffusion processes in composite porous media and their numerical integration by random walks: Generalized stochastic differential equations with discontinuous coefficients, Water Resources Research, 36:651-662, 2000.

Liu, H.H., C. Doughty, and G. S. Bodvarsson, An active fracture model for unsaturated flow and transport in fractured rocks, Water Resources Research, 34:2633-2646, 1998.

Liu, H.H., G. S. Bodvarsson, and L. Pan, Determination of particle transfer in random walk particle methods for fractured porous media, Water Resources Research, 36:707-713, 2000.

Maloszewski, P., and A. Zuber, Tracer experiments in fractured rocks: Matrix diffusion and the validity of models, Water Resources Research, 29:2723-2725, 1993.

Neretnieks, I., Diffusion in the rock matrix: An important factor in radionuclide retardation?, J. Geophys. Res. 85(B8):4379-4397, 1980.

Pan, L., H.H. Liu, M. Cushey, and G. S. Bodvarsson, DCPT V1.0 – New particle tracker for modeling transport in dual continua media, Users' manual. Report LBNL-42958, Lawrence Berkeley National Laboratory, Berkeley, CA, 2001.

Pruess, K., and T. N. Narasimhan, A practical method for modeling fluid and heat flow in fractured porous media. Soc. Pet. Eng. J. 25:14-26, 1985.

Semra, K.,P. Ackerer, and R. Mose, Three-dimensional groundwater quality modeling in heterogeneous media, in Water Pollution II: Modeling, Measuring and Prediction, pp.3-11, Comput. Mech., Billerica, Mass., 1993.

Sudicky, E. A., and E. O. Frind, Contaminant transport in fractured porous media: Analytical solutions for a system of parallel fractures, Water Resources Research, 18:1634-1642, 1982.

Tompson, A.F.B., and L.W. Gelhar, Numerical simulation of solute transport in three-dimensional, randomly heterogeneous porous media, Water Resources Research, 26:2541-2562,1990.

Tsang, Y. W., and C. F. Tsang, A particle-tracking method for advective transport in fractures with diffusion into finite matrix blocks. Water Resources Research, 37:831-835, 2001.

Uffink, G. J. M., A random-walk method for the simulation of macrodispersion in a stratified aquifer, in Relation of Groundwater Quality and Quantity, IAHS Publ., 146:103-114, 1985.

van Genuchten, M. Th., and F.N. Dalton, Models for simulating salt movement in aggregated field soils. Geoderma, 38:165-183, 1986.

Wu, Y. S., and K. Pruess, Numerical simulation of non-isothermal multiphase tracer transport in heterogeneous fractured porous media. Advances in Water Resources. 23:669-723, 2000.

Wu, Y. S., J. Liu, T. Xu, C. Haukwa, W. Zhang, H.H., Liu, and C.F. Ahlers, UZ flow models and submodels. Analysis/Model Report MDL-NBS-HS-000006 REV00G, CRWMS M&O, 2000.

Wu, Y.-S., K. Zhang, C. Ding, K. Pruess, E. Elmroth , and G. S. Bodvarsson. An Efficient Parallel-Computing Scheme for Modeling Nonisothermal Multiphase Flow and Multicomponent Transport in Porous and Fractured Media. Advances in Water Resources 2001 (Submitted).

Appendix A: Derivation of the general scheme of the particle-transfer probability

In the framework of the dual-continuum model, the mass of particles initially in continuum j will be partitioned into three portions after a duration [0, t]. They are:

(a) Mass entering the same continuum of neighboring cells (m^j_{out});

(b) Mass entering the other continuum of the same cell (m_{jk});

(c) Mass staying in the same continuum of the same cell (m^j_t).

Therefore, the particle-transfer probability, at which a single particle in continuum j at t = 0 will be in continuum k at time t, can be defined as the following ratio:

$$P_{jk} = \frac{m_{jk}}{m_{jk} + m^j_{out} + m^j_t} = \frac{m_{jk}}{m^j(0)} \qquad (A1)$$

where m^j (0) is the mass of particles initially in continuum j.

The mass-balance equation for the particles in continuum j at t = 0 for a given cell can be expressed as:

$$C_j(0)(Vol_j + Kd_j m_j) = C_j(t)(Vol_j + Kd_j m_j) + \int_0^t F_{jk}\, C_j(\tau)\, d\tau + \int_0^t Q_j C_j(\tau)\, d\tau \qquad (A2)$$

where C_j, Vol_j, Kd_j, and m_j are the concentration, volume of liquid, adsorption coefficient, and mass of rock in continuum j, respectively. F_{jk} and Q_j describe the strength of advection and dispersion/diffusion processes through the fracture-matrix interface and the interfaces to adjacent grid cells in continuum j, respectively. The detailed expressions of these two parameters are shown in Equations (3a) and (3b) for fracture continuum (j = f), and Equations (3d) and (3e) for matrix continuum (j = m), respectively. Both F_{jk} and Q_j are assumed to be constant within the time interval (0, t). Note that handling F_{jk} and Q_j in this way is equivalent to the way for representing the net mass flux through an interface in a finite-difference method. For example, the net mass flux from fracture continuum to matrix continuum can be expressed as (replacing j with f and k with m):

$$F_{fm} C_f - F_{mf} C_m = \max(q_{fm} A_{fm}, 0) C_f - \max(-q_{fm} A_{fm}, 0) C_m + \frac{D_m A_{fm}}{S_{fm}} [C_f - C_m] \qquad (A3)$$

In Equation (A3), the sum of first two terms on the right side represents the advection flux while the last term on the right side is simply the finite-difference approximation of the diffusion flux at the fracture-matrix interface.

Taking derivatives on both sides of Equation (A2) with respect to t, we have a first order ordinary differential equation:

$$\frac{dC_j(t)}{dt} + \frac{1}{\tau_j} C_j(t) = 0 \qquad \text{(A4)}$$

where, τ_j is the characteristic time of continuum j for the given cell, and is defined as :

$$\tau_j = \frac{Vol_j + Kd_j\, m_j}{F_{jk} + Q_j} \qquad \text{(A5)}$$

The solution of Equation (A4) is readily obtained as

$$C_j(t) = C_j(0)\ \exp\ (-t/\ \tau_j) \qquad \text{(A6)}$$

Therefore, the probability of a particle being transferred from continuum j to continuum k during (0, t) can be calculated as:

$$P_{jk} = \frac{F_{jk}\int_0^t C_j(\tau)d\tau}{C_j(0)\left(Vol_j + Kd_j\, m_j\right)} = \frac{F_{jk}}{Q_j + F_{jk}}\left[1 - \exp\left(-t/\tau_j\right)\right] \qquad \text{(A7)}$$

Note that, in the above derivation, we use t instead of Δt for symbolic simplicity. The t = 0 actually indicates the starting point of a time step. The particle-transfer probability from fracture continuum to matrix continuum defined in Equation (2a) are obtained by replacing t with Δt, j with f, and k with m in (A7), respectively. Expression (2b) can be obtained in the similar way.

Table 1 Parameters Used for the Transport Problem in a Parallel Fracture System

Parameter	Value
Molecular diffusion coefficient (D_m)	2.5×10^{-11} m^2 /s
Fracture spacing (2B)	1.0 m (Case 1) or 10.0 m (Case 2)
Fracture aperture (2b)	2×10^{-5} m
Retardation factor (R)	30
Volumetric Water content in matrix	0.1 m^3/m^3
Velocity in fracture	1.1574×10^{-5} m/s
Grid spacing	0.5 m
Matrix volume per cell	0.25 m^3 (Case 1) or 2.5 m^3 (Case 2)
Fracture volume per cell	0.5×10^{-5} m^3
Fracture-matrix interface area	0.5 m^2
Distance from the source of tracer to the observation point	36.5 m

Table 2 Parameters for the mountain-scale transport problem

Parameters	**Technetium** (Tc)	**Neptunium**(Np)
Molecular diffusion coefficient (m^2/s)	3.2×10^{-11}	1.6×10^{-10}
Adsorption coefficient K_d (cm^2/s)	0.0 for all fractures and matrix	4.0 for zeolitic matrix in CHn; 1.0 for vitric matrix and fault matrix in CHn; 1.0 for matrix in TSw; 0.0 for else

Note: CHn—Calico Hills non-welded unit; TSw—Tiva Canyon welded unit.

Figure Captions

Figure 1. An example showing that a dual-continuum approach (e.g., DCPT V1.0) may overestimate the early breakthrough in fractured porous media

Figure 2. Schematic of the propagation of a pulse in a fracture-matrix system with time. Parallel fractures separated by porous rock (upper portion). The distribution density function becomes wider and flatter over time (lower portion, t3 > t2 > t1)

Figure 3. Predicted breakthrough by DCPT v1.0, DCPT v2.0, and the analytical solution for Case 1 (1 m fracture spacing)

Figure 4. Predicted breakthrough by DCPT v1.0, DCPT v2.0, and the analytical solution for Case 2 (10 m fracture spacing)

Figure 5. The effects of fracture spacing on the breakthrough as a function of time.

Figure 6. The particle-transfer probabilities for both directions as a function of the particle's age (t_p) for Case 1 and Case 2. The fracture spacing affects the critical t_p at which the particle-transfer probability becomes independent of the particle's age. There exists a quadric relationship between the critical t_p and the fracture spacing.

Figure 7. Plan view of the three-dimensional numerical grid of the unsaturated zone of Yucca Mountain, showing the model domain, faults, underground tunnels, and several borehole locations.

Figure 8. Predicted relative mass breakthrough curves of a conservative tracer (Tc) arriving at water table using DCPT v1.0, DCPT v2.0, and T2R3D, respectively. The only difference between the two versions of DCPT is the scheme calculating the particle-transfer probabilities. Radioactive decay is ignored.

Figure 9. Predicted relative mass breakthrough curves of an adsorbing tracer (Np) arriving at water table using DCPT v1.0, DCPT v2.0, and T2R3D, respectively. The only difference between the two versions of DCPT is the scheme calculating the particle-transfer probabilities. Radioactive decay is ignored.

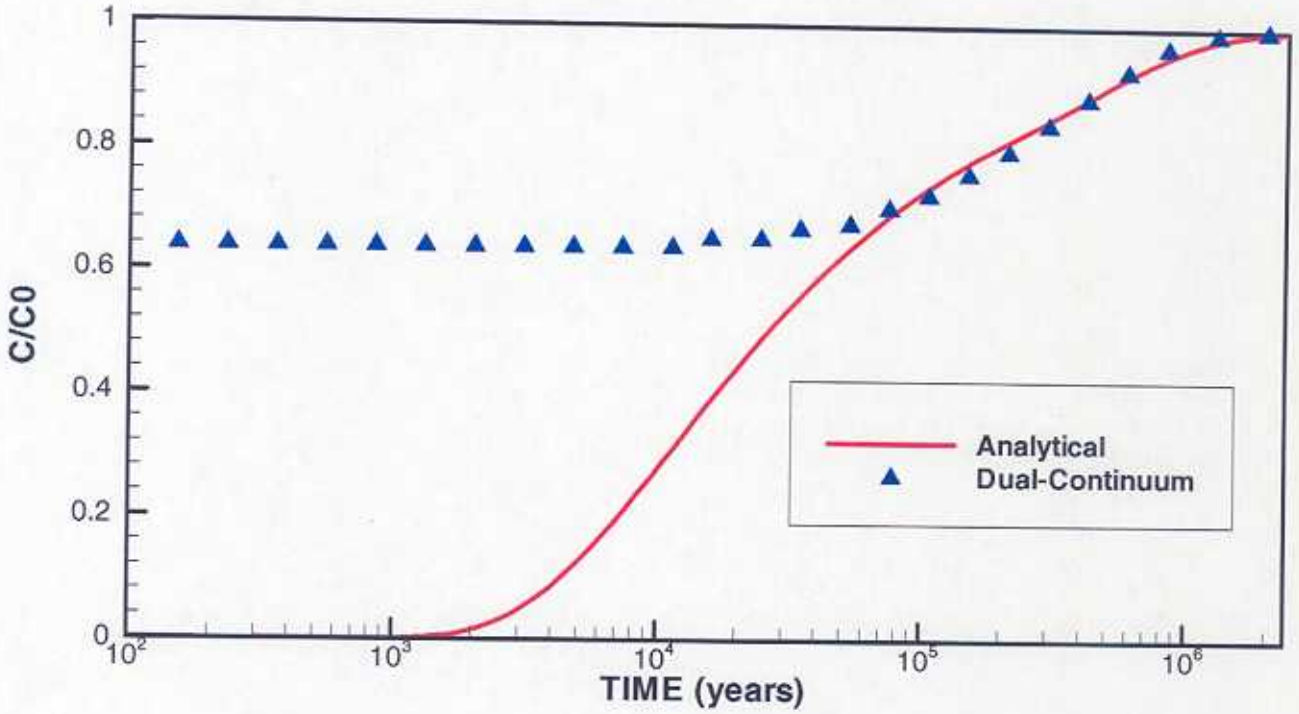
1
0.8
0.6
0.4
0.2
0
C/C0
10^2
10^3
10^4
10^5
10^6
TIME (years)
Analytical
Dual-Continuum

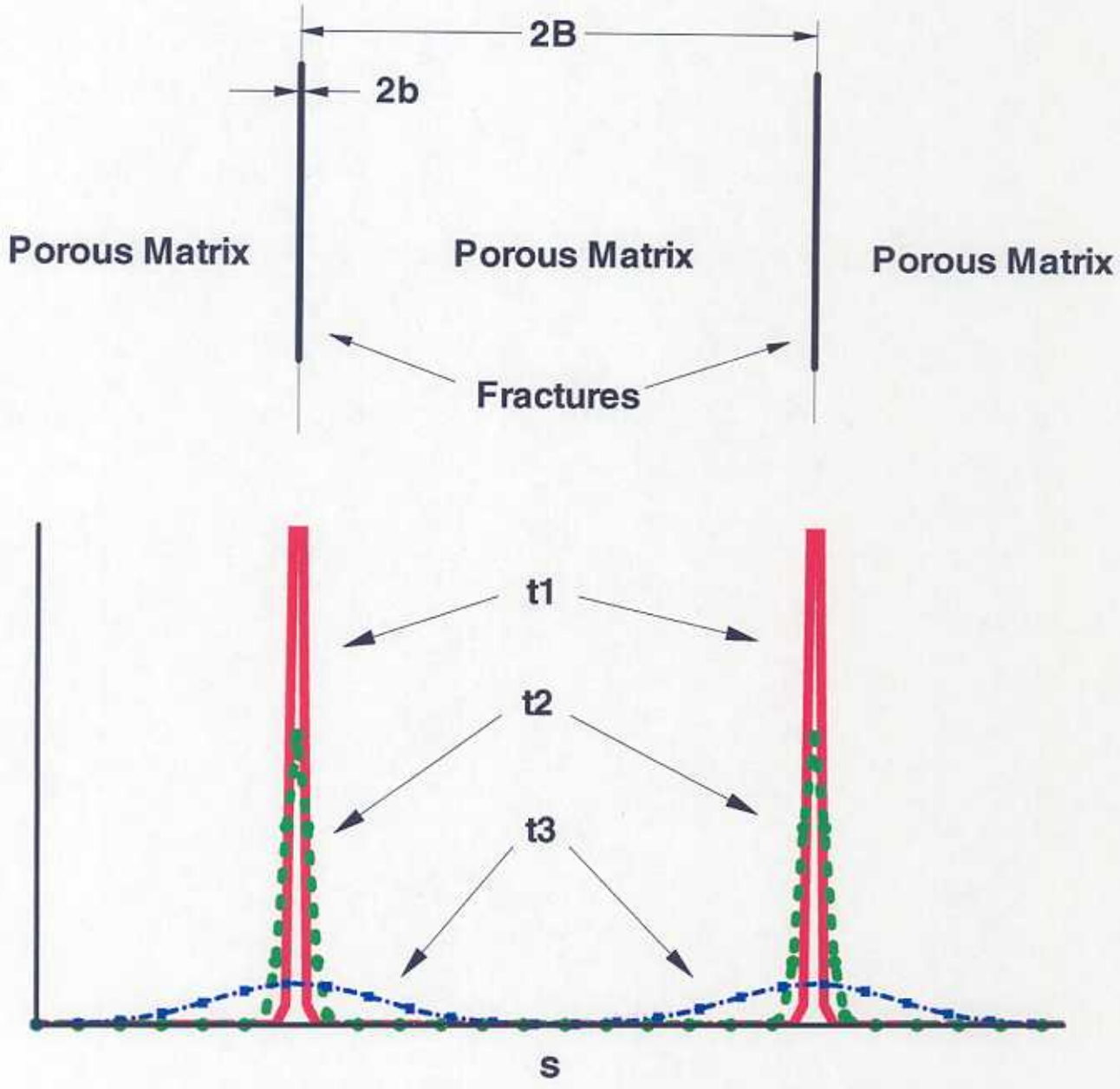
2B
2b
Porous Matrix
Porous Matrix
Porous Matrix
Fractures
t1
t2
t3
c
s

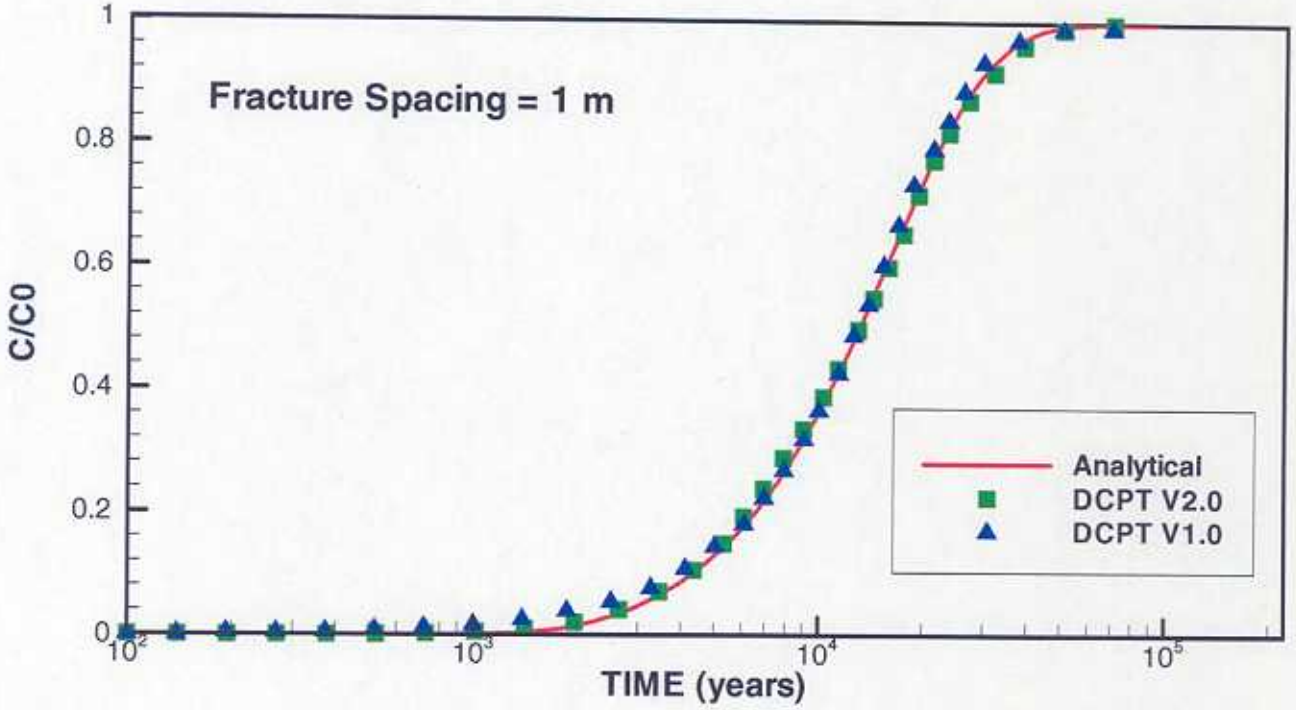
Fracture Spacing = 1 m
C/C0
TIME (years)
Analytical
DCPT V2.0
DCPT V1.0
0
0.2
0.4
0.6
0.8
1
10^2
10^3
10^4
10^5

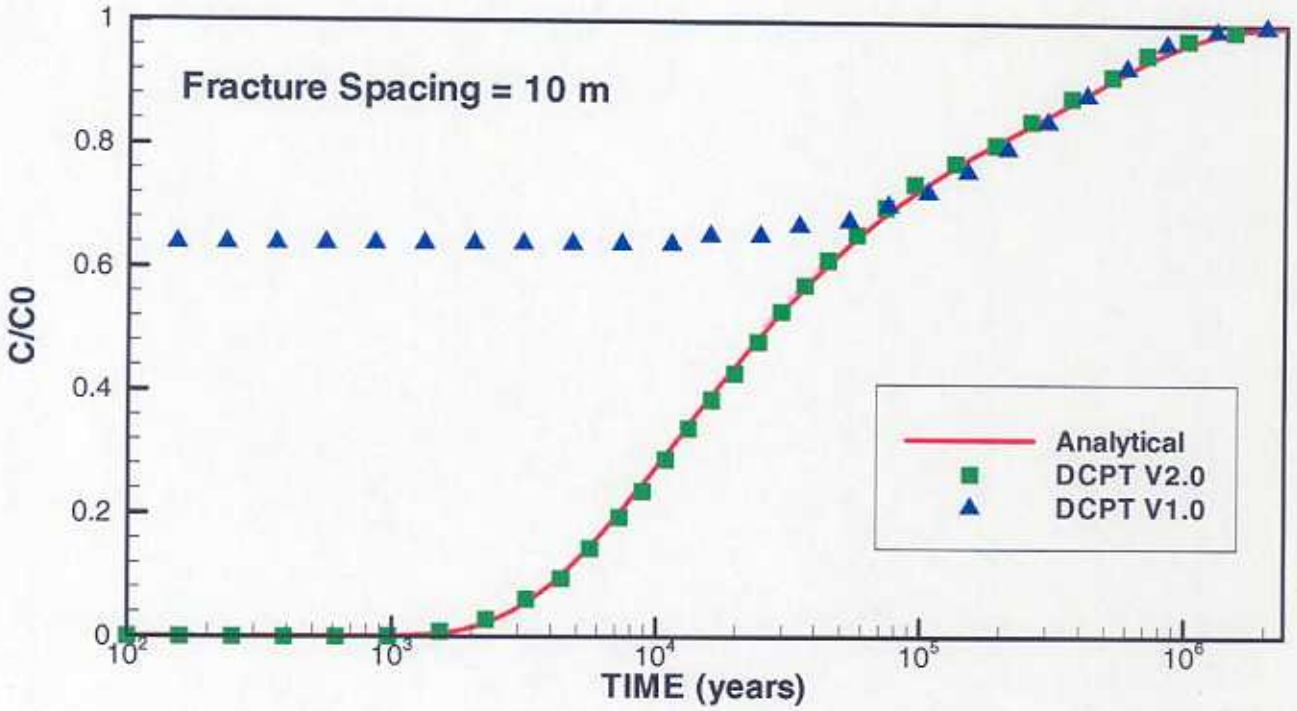
Fracture Spacing = 10 m
C/C0
TIME (years)
Analytical
DCPT V2.0
DCPT V1.0
0
0.2
0.4
0.6
0.8
1
10^2
10^3
10^4
10^5
10^6

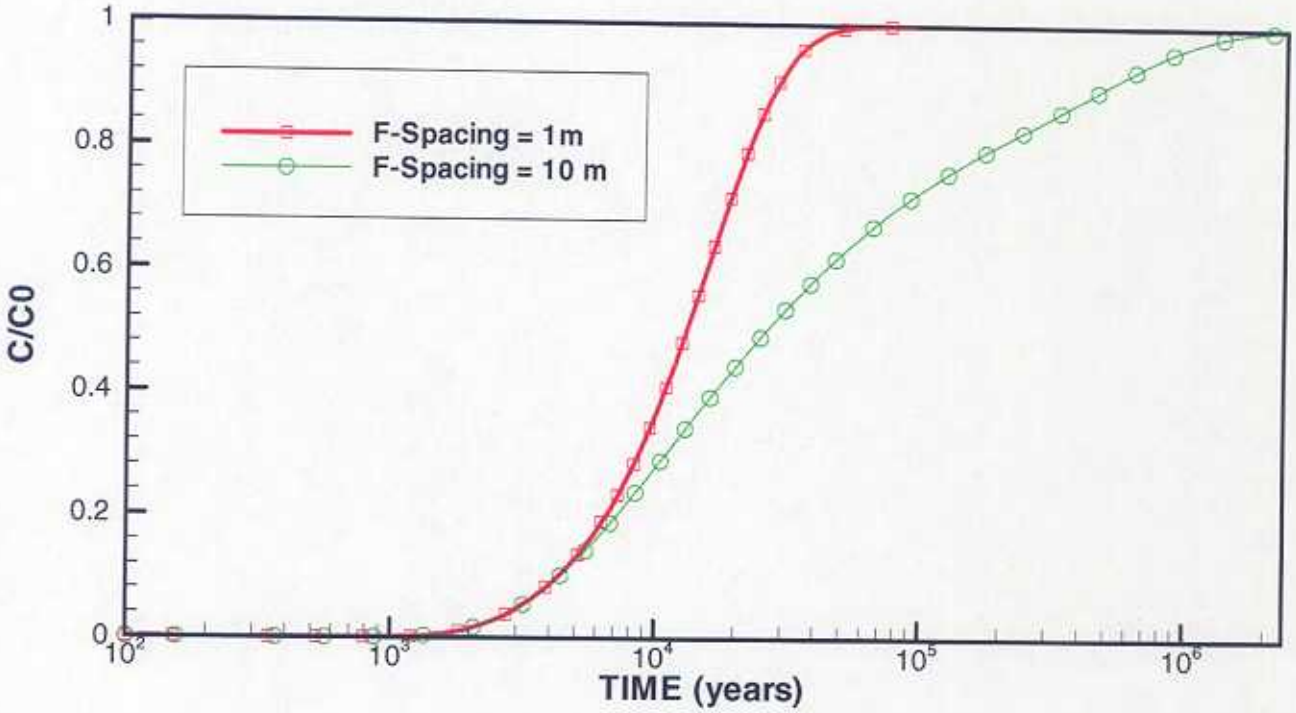
F-Spacing = 1m
F-Spacing = 10 m
C/C0
TIME (years)
0
0.2
0.4
0.6
0.8
1
10^2
10^3
10^4
10^5
10^6

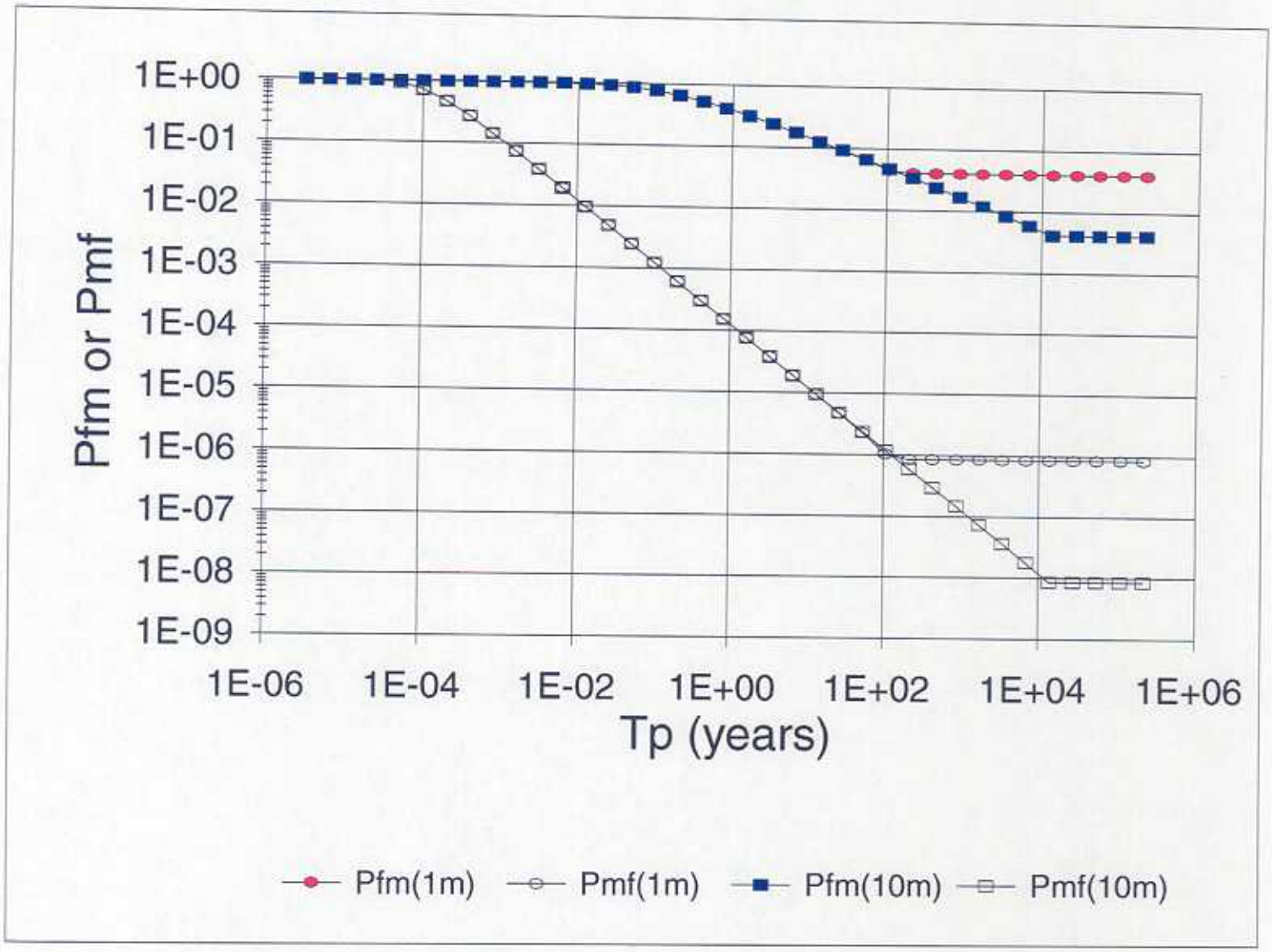
1E+00
1E-01
1E-02
1E-03
1E-04
1E-05
1E-06
1E-07
1E-08
1E-09
Pfm or Pmf
1E-06
1E-04
1E-02
1E+00
1E+02
1E+04
1E+06
Tp (years)
Pfm(1m)
Pmf(1m)
Pfm(10m)
Pmf(10m)

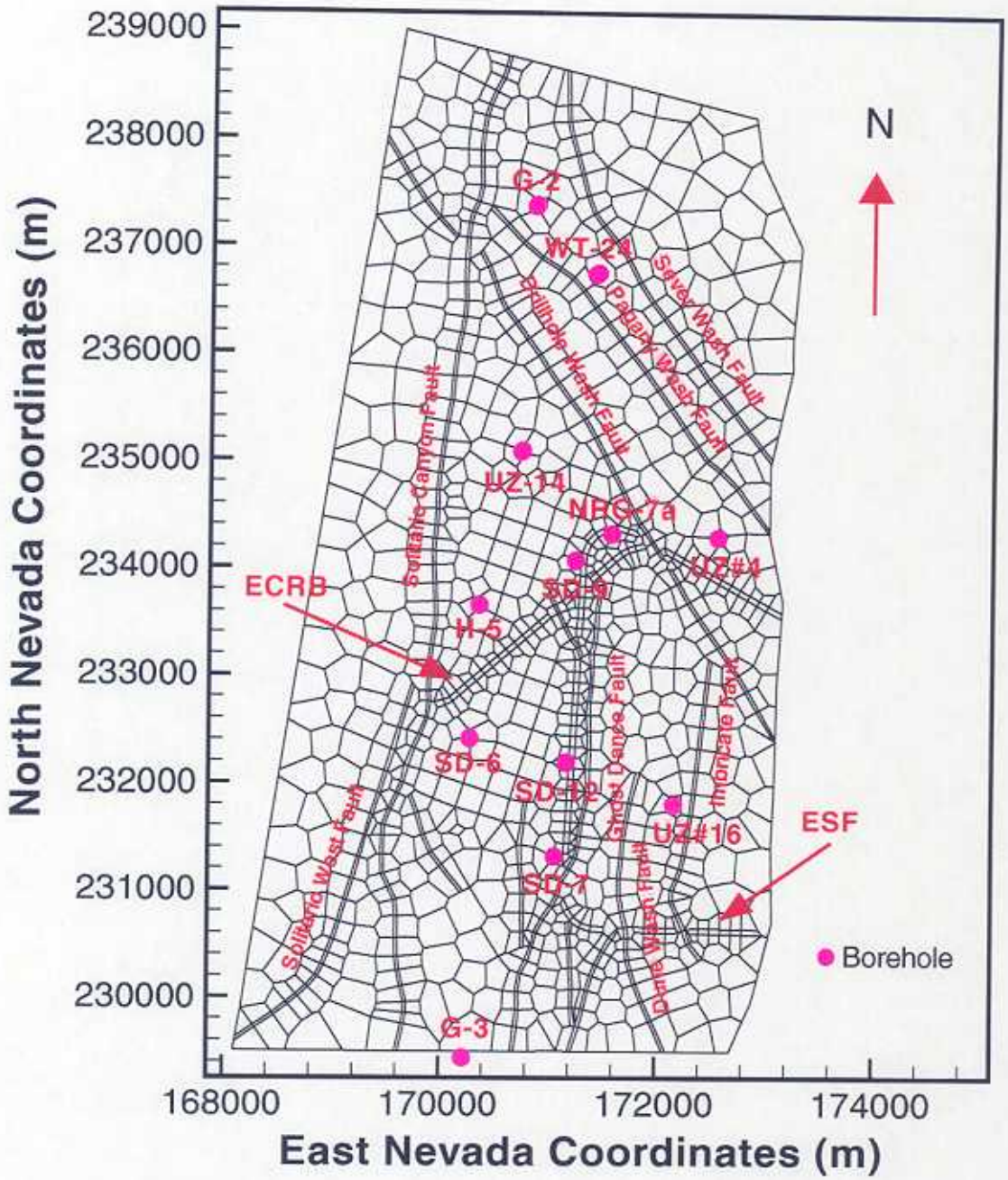
239000
238000
237000
236000
235000
234000
233000
232000
231000
230000
North Nevada Coordinates (m)
168000
170000
172000
174000
East Nevada Coordinates (m)
N
G-2
WT-24
Paintbrush Wash Fault
Silver Wash Fault
Drillhole Wash Fault
Solitario Canyon Fault
UZ-14
NRG-7a
UZ#4
SD-9
ECRB
H-5
SD-6
SD-12
Ghost Dance Fault
Imbricate Fault
UZ#16
ESF
SD-7
Solitario West Fault
Dune Wash Fault
G-3
Borehole

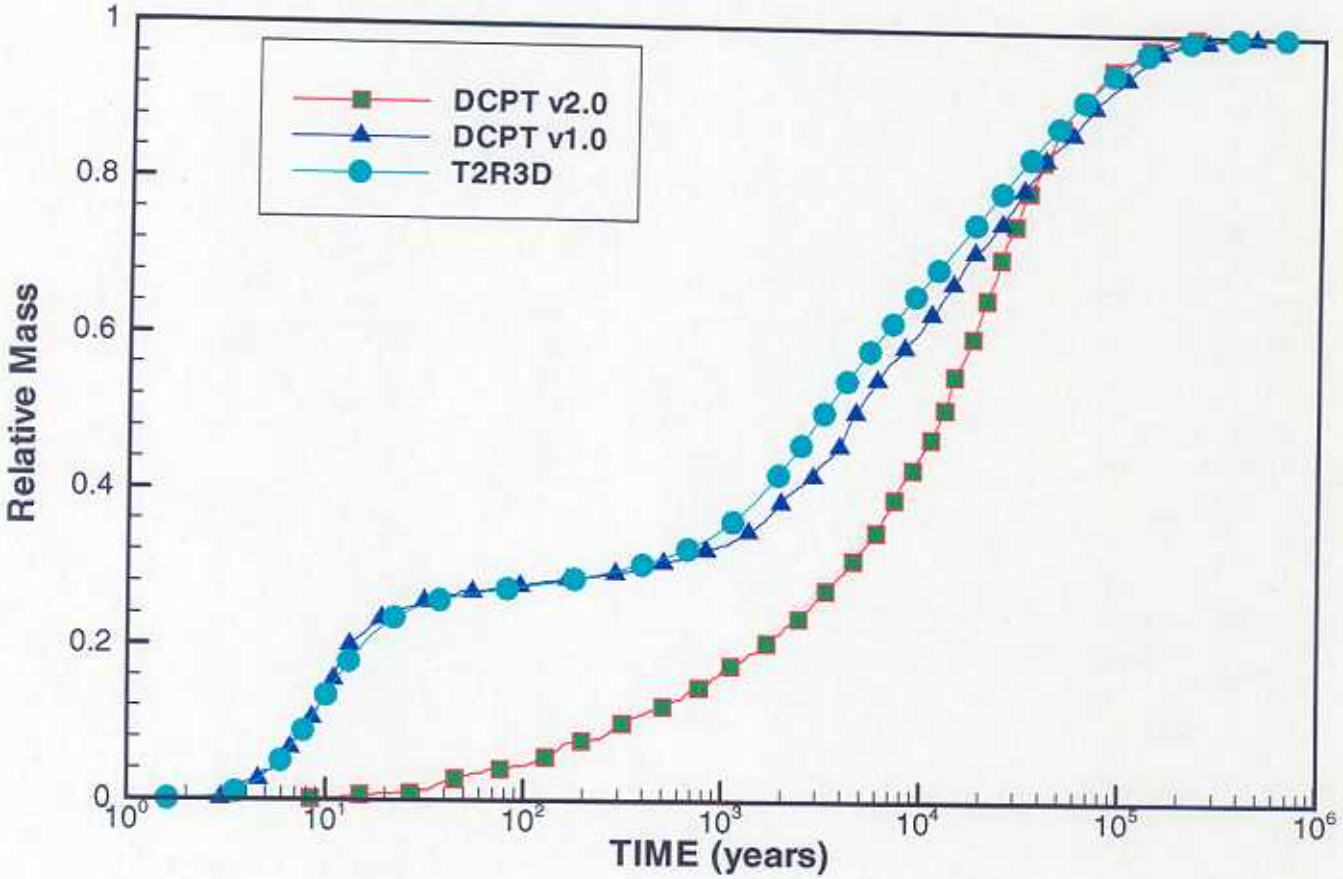
DCPT v2.0
DCPT v1.0
T2R3D
Relative Mass
TIME (years)
0
0.2
0.4
0.6
0.8
1
10^0
10^1
10^2
10^3
10^4
10^5
10^6